

Architectural analysis and predicted functional capability of the human latissimus dorsi muscle

Michael E. Gerling and Stephen H. M. Brown

Department of Human Health and Nutritional Sciences, University of Guelph, Guelph, ON, Canada

Abstract

The latissimus dorsi is primarily considered a muscle with actions at the shoulder, despite its widespread attachments at the spine. There is some dispute regarding the potential contribution of this muscle to lumbar spine function. The architectural design of a muscle is one of the most accurate predictors of muscle function; however, detailed architectural data on the latissimus dorsi muscle are limited. Therefore, the aim of this study was to quantify the architectural properties of the latissimus dorsi muscle and model mechanical function in light of these new data. One latissimus dorsi muscle was removed from each of 12 human cadavers, separated into regions, and micro-dissected for quantification of fascicle length, sarcomere length, and physiological cross-sectional area. From these data, sarcomere length operating ranges were modelled to determine the force–length characteristics of latissimus dorsi across the spine and shoulder ranges of motion. The physiological cross-sectional area of latissimus dorsi was $5.6 \pm 0.5 \text{ cm}^2$ and normalized fascicle length was $26.4 \pm 1.0 \text{ cm}$, indicating that this muscle is designed to produce a moderate amount of force over a large range of lengths. Measured sarcomere length in the post-mortem neutral spine posture was nearly optimal at $2.69 \pm 0.06 \mu\text{m}$. Across spine range of motion, biomechanical modelling predicted latissimus dorsi acts across both the ascending and descending limbs of the force–length curve during lateral bend, and primarily at or near the plateau region (where maximum force generation is possible) during flexion/extension and axial twist. Across shoulder range of motion, latissimus dorsi acts primarily on the plateau region and descending limbs of the force length curve during both flexion/extension and abduction/adduction. These data provide novel insights into the ability of the latissimus dorsi muscle to generate force and change length throughout the spine and shoulder ranges of motion. In addition, these findings provide an improved understanding of the spine and shoulder positions at which the force-generating capacity of this muscle can become jeopardized, and consequently how this may affect its spine-stabilizing ability.

Key words: biomechanics; lumbar spine; muscle architecture; sarcomere; shoulder.

Introduction

Latissimus dorsi is a unique muscle in terms of its anatomical design. It is a relatively thin, fan-shaped muscle, and is one of the largest in the body in surface area, covering a significant portion of the back (Fig. 1A). It assumes widespread medial attachments to the spinous processes of the lower six thoracic vertebrae, lumbar vertebrae, and sacrum, as well as to the ilium via the thoracolumbar fascia. In some cases, fibres can be found to attach to the lateral aspects of ribs 10–12. Muscle fibres then converge superiolaterally

toward the axilla, where they twist before inserting onto the anterior aspect of the proximal humerus. Functionally, due to its humeral attachment, the latissimus dorsi muscle is most often primarily considered a muscle with actions at the shoulder, contributing to adduction, extension, and medial rotation of the upper limb (Bogduk et al. 1998). Studies suggest that it also acts at the lumbar spine as an extensor and lateral bender of the back (Schultz & Andersson, 1981; McGill & Norman, 1986; McGill, 1987; Potvin et al. 1991; Goel et al. 1993; Guzik et al. 1996), although the muscle has received relatively little attention in this regard and some have suggested that it has no direct action on the lumbar vertebral column (Adams et al. 2002). Currently, functional interpretation of latissimus dorsi appears to be predominantly based on its gross anatomy; however, it is important to note that the action of a muscle cannot be attributed to this alone (Bogduk et al. 1998). Within a given muscle, contractile proteins within fibres

Correspondence

Stephen H. M. Brown, Department of Human Health and Nutritional Sciences, University of Guelph, Guelph, N1G 2W1, ON, Canada.

T: + 1 519 8244120, ext. 53651; F: + 1 519 7635902;

E: shmbrown@uoguelph.ca

Accepted for publication 24 May 2013

Article published online 13 June 2013

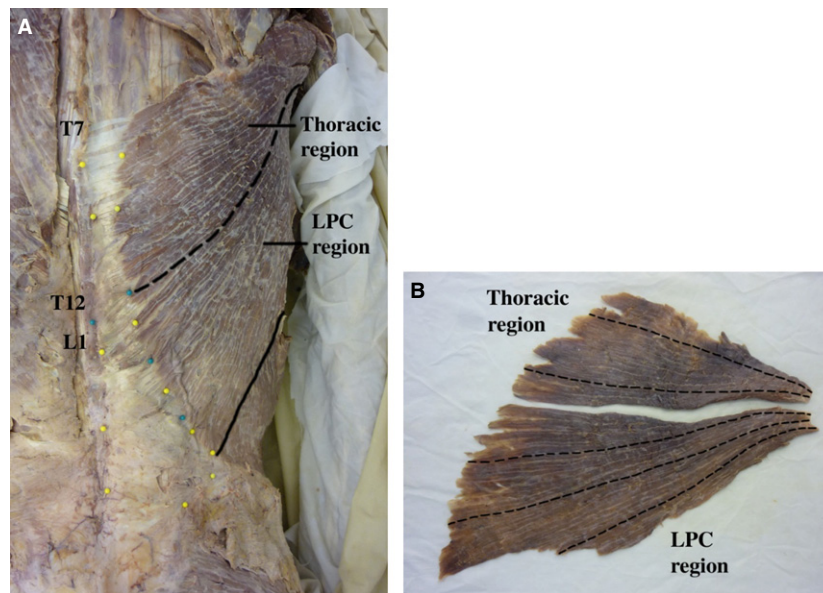


Fig. 1 (A) Regional division of the latissimus dorsi muscle. The muscle was divided at the level corresponding to the junction of the twelfth thoracic (T12) and first lumbar (L1) vertebrae (dashed line). Division at this location resulted in one region with attachments to the lower 6 thoracic vertebrae only (designated the thoracic region) and one region with attachments to the lumbar vertebrae, sacrum, and ilium of the pelvis, as well as lateral attachments to ribs 10–12 (designated the lumbar-pelvis-costal, LPC, region). Solid line represents the lateral border of the muscle. (B) Example of fascicle length measurements. Dashed lines represent location of fascicle length measurements for this particular muscle (note: fascicles were straightened to ensure accurate measurements). Due to the large variation in fascicle lengths that exists within latissimus dorsi, two measurements were taken from the thoracic region of each muscle, and three measurements were taken from each LPC region. Measurements from each region were then averaged. This was done in an effort to obtain an accurate representation of fascicle lengths within the muscle.

exhibit a characteristic in-series and in-parallel orientation. This structural design, defined as muscle architecture, is one of the most accurate predictors of muscle function (Lieber & Friden, 2001) and thus needs to be considered when determining the possible actions of a muscle. However, accurate, detailed knowledge of the architecture of the latissimus dorsi muscle is limited.

Architectural properties that are of particular functional relevance include muscle physiological cross-sectional area (PCSA) and normalized fascicle (i.e. fibre) length. PCSA represents the number of force-generating sarcomeres arranged in-parallel within a muscle and predicts its maximum force-producing capability (Powell et al. 1984). Normalized fascicle length represents the number of sarcomeres arranged in-series through a muscle and indicates its excursion potential (i.e. the range of lengths over which a muscle is capable of actively producing force) (Lieber & Friden, 2000). The greater the number of sarcomeres arranged in-series through a muscle, the greater the excursion potential, as each sarcomere is capable of accommodating a specific absolute length change based on the sarcomere force-length relationship. Thus, the number of sarcomeres changing length and acting in-series within a muscle can be summed to determine the overall range of lengths through which a muscle can generate force. Together, these architectural parameters describe the functional capacity of a muscle.

Biomechanical models designed to assess lumbar spine loading and stability rely heavily on architectural data, in particular muscle PCSA, to partition internal forces among the many different muscles and passive tissues of the lumbar spine (Brown & Gerling, 2012). Many of these models have incorporated the latissimus dorsi muscle into their analyses (McGill & Norman, 1986; McGill, 1987; Potvin et al. 1991; Goel et al. 1993; Cholewicki et al. 1995; Granata & Marras, 1995; Cholewicki & McGill, 1996; Guzik et al. 1996; Marras & Granata, 1997), despite the limited knowledge of its architectural properties. Thus, it is currently unclear whether these models have presented accurate representations of this muscle. Fascicle length and PCSA of the latissimus dorsi muscle have been reported previously by Bogduk et al. (1998); however, a limitation of that study was that these architectural parameters were quantified without accounting for potential variation in muscle fixation length. Not accounting for non-optimal fixed lengths introduces the risk of obtaining PCSA estimates of muscles in either lengthened or shortened states, leading to under- and over-estimations of these values, respectively (Brown & Gerling, 2012). To correct for length differences that occur during fixation and subsequently eliminate potential inaccuracies of PCSA estimations, sarcomere length measurements can be used to normalize fascicle length measurements (Lieber & Friden, 2000). Furthermore, measurement of sarcomere

length permits the estimation of sarcomere length operating ranges, providing insight into the mechanical function of a muscle through its range of motion (ROM). To our knowledge, the sarcomere length operating ranges of the human latissimus dorsi muscle across the spine range of motion are unknown. Therefore, the purpose of the present study was to quantify the architectural properties of the latissimus dorsi muscle, taking into account sarcomere length at fixed muscle lengths. In light of these new data, sarcomere length operating ranges were modelled to determine the ability of the latissimus dorsi muscle to generate force and change length throughout the spine ROM. In addition, due to the attachment of latissimus dorsi to the proximal humerus, it was necessary to consider how movement about the shoulder influences length changes of the latissimus dorsi muscle, and subse-

quently how this may affect its force-generating and stabilizing capacity at the spine. Therefore, sarcomere length operating ranges across the shoulder joint ranges of motion were also modelled.

Materials and methods

Twelve formaldehyde-fixed human cadavers (nine male, three female) were studied: mean \pm SD age = 63.0 ± 11.0 years, range = 45–83 years (Tables 1 and 2). Eight of the cadavers were embalmed in the approximate anatomical position, while the remaining four were embalmed with the arms abducted approximately 100° relative to the lateral aspect of the body. None of the cadavers had any visible spinal-related injury or pathology. Use of cadavers for the present study was approved by the University Research ethics board, as well as the Chief Coroner of Ontario.

Table 1 Architectural properties of the human latissimus dorsi muscle.

	Age	Gender	Mass (g)	Fascicle length (cm)	Sarcomere length (μm)	Sarcomere number	Normalized fascicle length (cm)	PCSA (cm^2)
LD1 (Whole)	73	M	164.5	25.1	2.57	98 141	26.5	5.4
LD1 (T)			48.3	24.2	2.71	89 336	24.1	1.8
LD1 (LPC)			116.2	26.0	2.43	106 947	28.9	3.6
LD2 (Whole)	71	M	157.4	22.8	2.63	86 203	23.3	5.9
LD2 (T)			51.8	19.9	2.55	77 782	21.0	2.2
LD2 (LPC)			105.6	25.7	2.72	94 624	25.5	3.7
LD3 (Whole)	74	M	121.4	26.1	2.45	105 983	28.6	3.7
LD3 (T)			37.6	22.8	2.41	94 811	25.6	1.3
LD3 (LPC)			83.8	29.3	2.50	117 156	31.6	2.4
LD4 (Whole)	48	F	171.5	25.2	2.79	90 226	24.4	6.1
LD4 (T)			54.8	21.5	2.75	78 087	21.1	2.3
LD4 (LPC)			116.7	28.9	2.83	102 364	27.6	3.8
LD5 (Whole)	UK	M	120.0	27.2	2.69	102 223	27.6	3.9
LD5 (T)			45.5	25.0	2.89	86 642	23.4	1.8
LD5 (LPC)			74.5	29.5	2.50	117 804	31.8	2.1
LD6 (Whole)	83	M	177.7	24.6	2.68	92 281	24.9	6.2
LD6 (T)			54.1	23.1	2.82	82 025	22.1	2.2
LD6 (LPC)			123.6	26.0	2.53	102 537	27.7	4.0
LD7 (Whole)	63	M	260.5	31.2	2.98	104 825	28.3	8.1
LD7 (T)			87.9	29.6	3.03	97 661	26.4	3.0
LD7 (LPC)			172.6	32.9	2.94	111 989	30.2	5.1
LD8 (Whole)	61	M	190.1	28.9	2.71	107 031	28.9	5.7
LD8 (T)			48.5	27.4	2.82	97 180	26.2	1.7
LD8 (LPC)			141.6	30.4	2.60	116 883	31.6	4.0
Mean \pm SEM (whole muscle)	68.0 \pm 11.0		170.4 \pm 15.6	26.4 \pm 1.0	2.69 \pm 0.06	98 364 \pm 2806	26.6 \pm 0.8	5.6 \pm 0.5

SEM indicates standard error of the mean ($n = 8$). Age is indicated as mean \pm SD. UK indicates unknown.

Data in bold represent whole muscle architectural data; data not in bold represent regional architectural data.

Sarcomere number represents in-series estimate; PCSA indicates physiological cross-sectional area. LD, latissimus dorsi; T, thoracic region; LPC, lumbar-pelvis-costal region.

Table 2 Architectural properties of human latissimus dorsi muscle when fixed with the arms abducted approximately 100° from the lateral aspect of the body.

Muscle	Age	Gender	Mass (g)	Fascicle length (cm)	Sarcomere length (μm)
LDS1 (Whole)	63	F	127.3	32.3	2.55
LDS1 (T)			32.1	29.8	2.30
LDS1 (LPC)			95.2	34.7	2.80
LDS2 (Whole)	63	F	175.4	33.1	2.61
LDS2 (T)			42.4	31.2	2.68
LDS2 (LPC)			133.0	35.0	2.54
LDS3 (Whole)	58	M	119.7	31.0	2.71
LDS3 (T)			36.6	28.8	2.54
LDS3 (LPC)			83.1	33.2	2.87
LDS4 (Whole)	45	M	349.9	32.4	2.70
LDS4 (T)			115.7	31.5	2.69
LDS4 (LPC)			234.2	33.4	2.71
Mean ± SEM (whole muscle)	57.3 ± 8.5		193.0 ± 53.7	32.2 ± 0.4	2.64 ± 0.04

SEM indicates standard error of the mean ($n = 4$). Age is indicated as mean ± SD.

Data in bold represent whole muscle architectural data.

LDS indicates latissimus dorsi muscles that were fixed in a stretched state (cadavers were embalmed with arms abducted approximately 100° relative to lateral aspect of body). T, thoracic region; LPC, lumbar-pelvis-costal region.

Again, for eight of the samples, muscles were fixed, while attached to the skeleton, with the cadavers in the approximate anatomical position. One muscle from each cadaver was then removed fully intact and micro-dissected, ensuring that all tendon, connective tissue, and adipose were removed. Following dissection, latissimus dorsi muscles were thoroughly inspected to ensure that no visible defect or pathology existed. Each muscle was then divided into two regions based on its attachments to the spine, at the level corresponding to the junction of the twelfth thoracic and first lumbar vertebrae (Fig. 1A). Division at this location resulted in one region with attachments to the lower six thoracic vertebrae only (designated the thoracic region), and one region with attachments to the lumbar vertebrae, sacrum, ilium of the pelvis, and lateral surfaces of ribs 10–12 (designated the lumbar-pelvis-costal, LPC, region). This was done for the purposes of determining whether there was specialization of muscle architecture within the latissimus dorsi muscle. Division of the muscle at this location also resulted in the maintenance of more homogeneous fascicle lengths within each region.

Following division of the muscle, each region was weighed (resolution 0.01 g) to determine mass, and fascicle lengths within each region were measured (Fig. 1B) with a digital calliper (resolution 0.01 mm). A minimum of three small fibre bundles were dissected from each muscle region, and sarcomere length was measured using laser diffraction at multiple locations (at least three locations, randomly selected) along each bundle (Lieber et al. 1990). The number of sarcomeres within each muscle region was calculated by dividing the measured fascicle length (converted to μm) by the average measured sarcomere length. Measured fascicle lengths were then normalized using the following equation:

$$Lf_n(\text{cm}) = \frac{Lf_m(\text{cm}) * Ls_o(\mu\text{m})}{Ls_m(\mu\text{m})} \quad (1)$$

where, Lf_n = normalized fascicle length, Lf_m = measured fascicle length, Ls_m = measured sarcomere length, Ls_o = optimal sarco-

mere length for human muscle (2.70 μm) (Walker & Schrodt, 1974).

PCSA for each region was then calculated using the following formula:

$$\text{PCSA}(\text{cm}^2) = \frac{M(\text{g}) * \cos(\theta)}{\rho(\text{g}/\text{cm}^3) * Lf_n(\text{cm})} \quad (2)$$

where M = muscle mass, Lf_n = normalized fascicle length, θ = pennation angle (0° for the latissimus dorsi muscle), and ρ = density of muscle fixed in 37% formaldehyde (1.112 g cm⁻³) (Ward & Lieber, 2005).

Whole muscle architectural properties for each muscle were determined as follows: PCSA of each region was summed to obtain whole muscle PCSA (as the two regions act in-parallel during force production); measured fascicle length, sarcomere length, in-series sarcomere number, and normalized fascicle length were calculated as weighted averages across both regions. All values are reported as mean ± SE of the mean (SEM), unless otherwise stated. PCSA, sarcomere length and normalized fascicle length were compared between regions using paired Student's t -tests ($\alpha = 0.05$).

Length changes of the latissimus dorsi muscle were then modelled across the full ROM of the spine. Origin and insertions of the muscle were taken from the model, representing a 50th percentile male, of Cholewicki & McGill (1996). Latissimus dorsi was modelled as consisting of two separate lines of action (representing thoracic and LPC regions), with corresponding skeletal attachments to L1 and the ilium of the pelvis, respectively. These lines of action define the muscle moment arm about each lumbar spine joint. To simulate the length change of the LPC region of latissimus dorsi as the spine moves through its ROM, its superior attachment to the humerus was rotated with the skeleton through the ROM of all the vertebral levels to which it is attached (T7–8 to L5–S1 intervertebral levels) about each anatomic spine axis (flexion, 75°; extension 44°; lateral

bend, 71° each ipsilateral and contralateral; axial twist, 32° each ipsilateral and contralateral), while the spine and pelvic attachments remained fixed. Ranges of motion and distribution of motion among the intervertebral levels, were estimated from values previously published in the literature (White & Panjabi, 1990; McGill, 2002). Length change of the thoracic region of the latissimus dorsi was modelled similarly, but only across the spine ROM between T7–8 and T12–L1. Latissimus dorsi length changes were also modelled across shoulder flexion/extension and abduction/adduction ranges of motion, using origin and insertion coordinates (defining the muscle line of action) from the SIMM model, again representing a 50th percentile male (Delp & Loan, 1995) and ranges of motion from the American Academy of Orthopaedic Surgeons (Namdari et al. 2012) [from the anatomical position: flexion, 167°; extension, 62°; abduction, 184°; adduction, 50° (adduction ROM was not provided in the literature from the anatomical position so it was estimated)].

Relative muscle length changes were calculated from the model data, which permitted the estimation of sarcomere length changes across the spine and shoulder ROM (assuming that the cadaveric-measured sarcomere lengths correspond to a neutral spine and arm anatomical position). Sarcomere length ranges were then plotted with respect to the well known sarcomere force–length relationship (Gordon et al. 1966) (adjusted here for human muscle actin filament lengths; Walker & Schrodt, 1974).

The additional four human cadavers were obtained having been embalmed with the arms abducted approximately 100° relative to the lateral aspect of the body, thus resulting in the latissimus dorsi muscle being fixed in a lengthened state (Table 2). Fascicle and sarcomere length measurements were obtained as described above; however, these muscles were not included when modelling muscle length changes and sarcomere length operating ranges across spine and shoulder ROM. The purpose of examining these four additional samples was to compare sarcomere lengths of latissimus dorsi muscles fixed in a stretched position with those fixed in the anatomical position, thus providing insight into sarcomere length changes of latissimus dorsi during whole muscle lengthening.

Results

Architectural properties of each latissimus dorsi muscle fixed in the anatomical position are shown in Table 1. Normalized fascicle length, indicating excursion potential, ranged from 23.3 to 28.9 cm (mean = 26.6 ± 0.8 cm). Muscle PCSA, indicating maximum isometric force-generating capability, ranged from 3.7 to 8.1 cm² (mean = 5.6 ± 0.5 cm²).

Regional normalized fascicle length and muscle PCSA are plotted in Fig. 2. Recall that the purpose of dividing the muscle into regions was to determine whether there was regional architectural specialization within the latissimus dorsi muscle. Based on the regional analysis, it is clear that the majority of the force-generating capability of latissimus dorsi lies within the LPC region of the muscle; on average, the LPC region constituted 64% of the total PCSA of the muscle, exhibiting a PCSA of 3.6 ± 0.3 cm², whereas the thoracic region constituted only 36% of whole muscle PCSA with an average PCSA of 2.0 ± 0.2 cm² ($P < 0.0001$). Normalized fascicle lengths were also significantly longer in the LPC region compared with the thoracic region

($P < 0.001$), whereas measured sarcomere lengths were not different between the regions ($P = 0.81$).

Regional normalized fascicle length and muscle PCSA for each muscle were averaged and summed, respectively, to obtain whole muscle architectural properties (Table 1). From these results, it is evident that the latissimus dorsi muscle is specialized, relative to the other spine muscles, for moderate force production (PCSA = 5.6 ± 0.5 cm²) and high excursions (normalized fascicle length = 26.6 ± 0.8 cm); that is, it is capable of generating a relatively moderate amount of force over a large range of lengths.

In the post-mortem spine posture, mean sarcomere length of the latissimus dorsi muscle was 2.69 ± 0.06 μ m (Table 1). Predicted sarcomere length operating ranges across the three anatomic axes of spine motion and two anatomic axes of shoulder motion are shown in Fig. 3. Across the three anatomic spine axes, the largest sarcomere length operating range was predicted in lateral bend; however, sarcomeres within the LPC region have a substantially larger operating range through the range of ipsilateral to contralateral bend (1.64–3.3 μ m) than those within the thoracic region (2.41–3.21 μ m) (Fig. 3A). Nonetheless, these ranges indicate that both thoracic and LPC fibres act on the ascending and descending limbs of the force–length curve during lateral bend, where force-generating capability is impaired. The predicted sarcomere length operating ranges in flexion/extension and axial twist are substantially narrower than in lateral bend, with fibres from both thoracic and LPC regions acting primarily at or near the plateau region of the force–length curve, indicating that latissimus dorsi is able to produce maximum or near maximum force across these two axes of spine motion (Fig. 3A). Through shoulder ROM, predicted sarcomere length operating ranges are similar in flexion/extension and abduction/adduction of the arm at the shoulder joint, with fibres from both regions starting at or near the plateau region of the

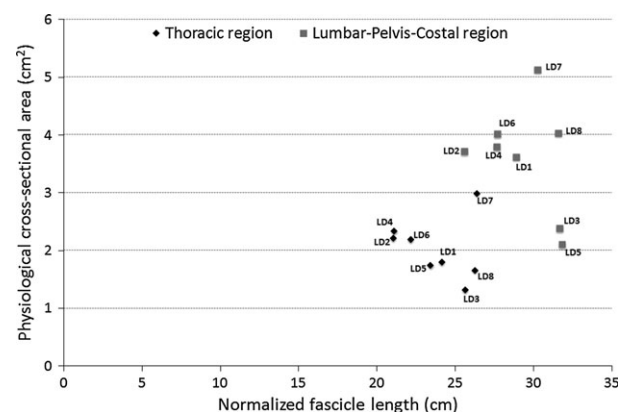


Fig. 2 Scatterplot of regional PCSA and normalized fascicle length for each latissimus dorsi muscle. The lumbar-pelvis-costal region has greater overall force-generating capacity and excursion potential than the thoracic region.

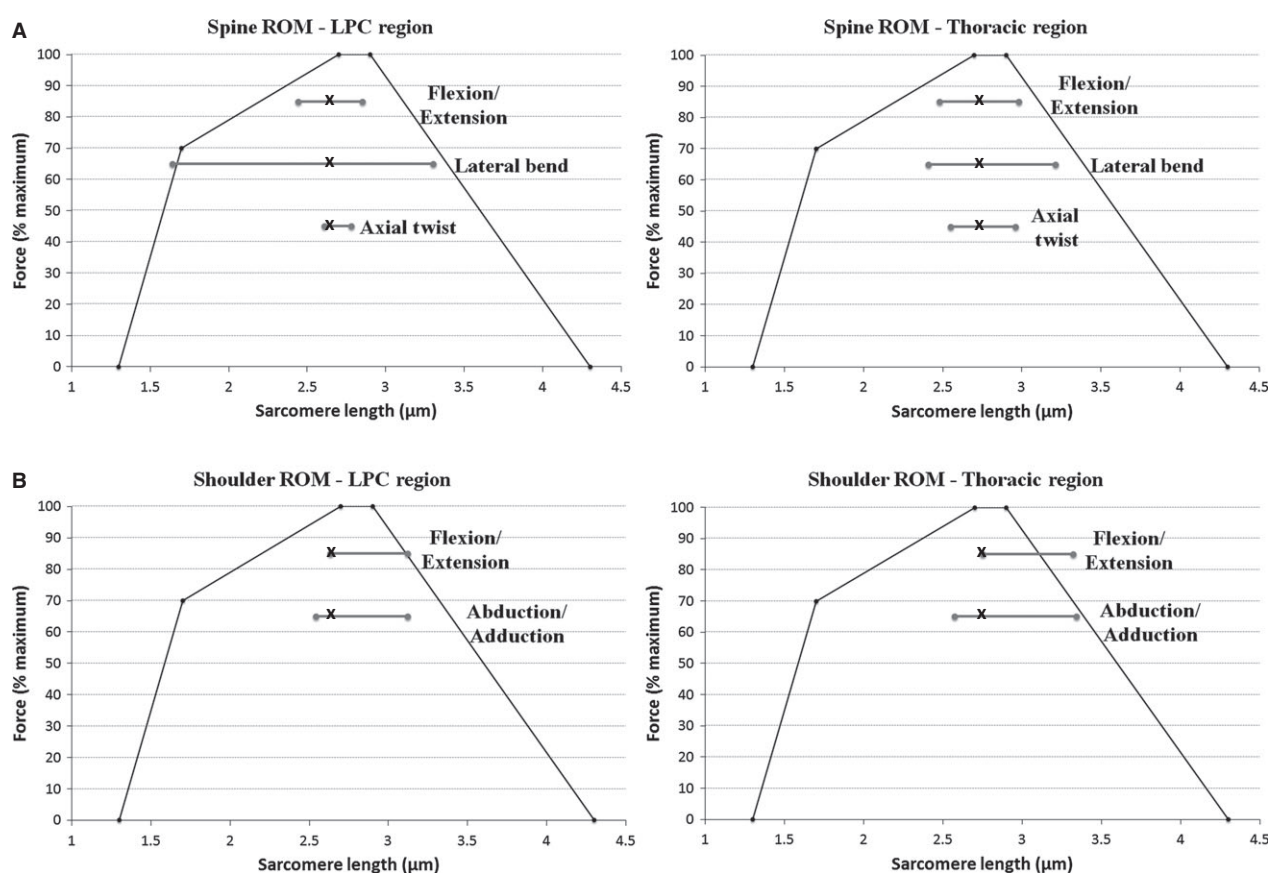


Fig. 3 (A) Predicted sarcomere length operating ranges (represented by horizontal lines) for the thoracic and lumbar-pelvis-costal (LPC) regions of latissimus dorsi across the three anatomic axes of spine motion. The bold 'x' on each line represents the neutral posture sarcomere length. Thoracic and LPC fibres of latissimus dorsi are at or near the plateau region of the force length curve in flexion/extension and axial twist. Fibres from both regions are long in contralateral bend, whereas fibres from the LPC region shorten substantially during ipsilateral bend. (B) Predicted sarcomere length operating ranges for the thoracic and LPC regions of latissimus dorsi across two of the three anatomic axes of shoulder motion. Thoracic and LPC fibres are long in flexion and abduction of the arm at the shoulder joint. The force-length relationship is estimated for human muscle assuming a myosin and actin filament length of 1.6 and 1.3 μm , respectively. Percent force values were taken from the force-length relationship for human skeletal muscle predicted by Rassier et al. (1999).

force-length curve and extending onto the descending limb during flexion, extension, and abduction (Fig. 3B).

Regional and whole muscle fascicle and sarcomere length measurements of latissimus dorsi muscles fixed in a stretched state are shown in Table 2. As expected, fascicle length of latissimus dorsi in a stretched state (32.2 ± 0.4 cm) was substantially longer than that of latissimus dorsi in a 'non-stretched' state (26.4 ± 1.0 cm); however, there was no corresponding increase in sarcomere length of the stretched muscles. Unexpectedly, the sarcomere length of the stretched latissimus dorsi muscles (2.64 ± 0.04 μm) was virtually the same as that of the 'non-stretched' muscles (2.69 ± 0.06 μm). Due to the unexpected sarcomere lengths of the stretched latissimus dorsi muscles, it was determined that normalized fascicle length and PCSA of these muscles could not be calculated reliably. For the same reason, these muscles were not included when modelling sarcomere length operating ranges of latissimus dorsi.

Discussion

This is the first study to interpret the function of the human latissimus dorsi muscle based on detailed architectural parameters. In particular, this study provides the first reports of serial sarcomere number and lengths for the latissimus dorsi muscle, indicating the range of muscle lengths over which this muscle is capable of producing active force. The availability of such data permits the estimation of sarcomere length operating ranges, allowing for the determination of the force-length characteristics of latissimus dorsi throughout the spine and shoulder ROM. Together with information regarding the force-generating capability of a muscle, these data are of fundamental importance for biomechanical modelling analyses of muscle and joint forces at the spine and shoulder.

The architecture of a muscle is one of the most accurate predictors of its function (Lieber & Friden, 2001). The PCSA

of a muscle is directly proportional to maximum force-generating potential (Powell et al. 1984), and normalized fascicle length is proportional to excursion potential (Bodine et al. 1982). The latissimus dorsi muscle was found to have a relatively moderate PCSA ($5.6 \pm 0.5 \text{ cm}^2$) and large normalized fascicle length ($26.6 \pm 0.8 \text{ cm}$) (Table 1). These architectural properties provide important details regarding sarcomere organization within latissimus dorsi, and thus its functional capacity. While latissimus dorsi is one of the largest muscles in the body in terms of surface area, its PCSA reveals that there are a relatively low number of sarcomeres arranged in-parallel within the muscle, which indicates that it is capable of generating only a moderate amount of force. Conversely, the large normalized fascicle length of latissimus dorsi indicates that it is composed of a high number of sarcomeres arranged in-series, each capable of accommodating a specific absolute length change based on the sarcomere force-length relationship, which when summed give this muscle as a whole the ability to undergo large length changes. Therefore, while latissimus dorsi has a relatively moderate force-generating capacity, it is capable of producing force over a wide range of lengths. However, it is interesting to note that this excursion potential is used only across a limited range of its joint motions. For example, muscle fascicles undergo predicted length changes up to 16.7 cm through the range of ipsilateral to contralateral bend of the spine, but only up to 3.4 cm through the range of ipsilateral to contralateral twist and 4.2 cm through the range of flexion to extension. This greater excursion length through lateral bend, as compared with axial twist and flexion/extension, is due to a combination of longer mean moment arms and a greater overall range of motion about this axis. Throughout motion of the shoulder, fascicle length changes are modest, undergoing changes up to 6.9 cm during full flexion to extension and 8.3 cm during abduction/adduction. Therefore, these data suggest that while latissimus dorsi is designed to produce a moderate amount of force over a large range of lengths, its functional capacity is also dependent upon the functional demands of its associated joints. In some situations, such as during lateral bend of the spine or abduction/adduction of the shoulder, the primary function of latissimus dorsi may be to utilize its excursion potential and assist with movement of a given joint(s), whereas in other cases, such as during axial twist of the spine, its main function may be to contribute to the stability of its associated joint(s), and much less so in providing motion.

The architectural design of latissimus dorsi demonstrates that its functional capacity is quite different than that of other major trunk muscles, particularly in terms of its excursion potential (Fig. 4). While the latissimus dorsi muscle has a force-generating capacity (PCSA = $5.6 \pm 0.5 \text{ cm}^2$) similar to that of longissimus and iliocostalis (5.9 ± 1.12 and $4.1 \pm 0.85 \text{ cm}^2$, respectively; Delp et al. 2001), the length range over which it is capable of producing active force is

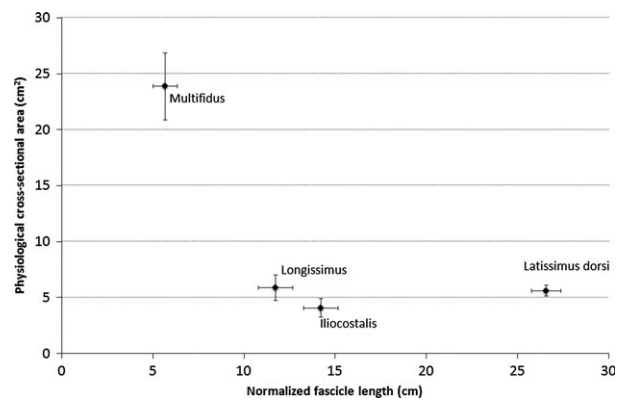


Fig. 4 Scatter plot of PCSA and normalized fascicle lengths of latissimus dorsi and select trunk muscles. Large PCSA indicates large force-generating capability, and a long normalized fascicle length indicates the ability to produce force over a wide range of lengths. These data illustrate that the latissimus dorsi muscle has an extremely high excursion potential compared with other trunk muscles. Data on longissimus and iliocostalis muscles were reported by Delp et al. (2001); data on multifidus were reported by Ward et al. (2009). Data are plotted as mean \pm SEM.

substantially larger (normalized fascicle length = 26.6 ± 0.8 , 11.7 ± 0.94 , and $14.2 \pm 0.94 \text{ cm}$, respectively; this study and Delp et al. 2001). Conversely, the multifidus muscle is composed of relatively short fibres and thus has a substantially lower excursion potential (normalized fascicle length = $5.7 \pm 0.65 \text{ cm}$; Ward et al. 2009) than latissimus dorsi; however, the latissimus dorsi muscle is capable of producing relatively little force in comparison to the multifidus muscle (PCSA = $23.9 \pm 3.0 \text{ cm}^2$; Ward et al. 2009). With a relatively moderate PCSA and large normalized fascicle length, the architecture of latissimus dorsi is somewhat opposite to that of multifidus; as such, one might infer that its role in spine function is also opposite to that of multifidus. However, it must be noted that to interpret function relative to the spine or another skeletal joint, muscle moment arms must be considered as important indicators of moment-generating and spine-stabilizing potential (Brown & Potvin, 2007). Importantly, the length change that a muscle experiences as it travels through its range of motion is highly dependent upon its geometrical line of action (defining its moment arms) about all of the joints that it crosses (Lieber & Bodine-Fowler, 1993). Thus, the operating ranges determined here are a combined function of the measured neutral cadaveric sarcomere lengths, the modelled line of actions with respect to each lumbar spine joint and the glenohumeral joint, and the ranges of motion employed from population averages. Finally, without knowing the sarcomere length operating ranges of longissimus, iliocostalis, and multifidus across the spine ROM, it is difficult to assess accurately the potential roles of these muscles in spine function compared with that of the latissimus dorsi muscle.

Due to the widespread attachments of latissimus dorsi to the thoracic and lumbar vertebrae, it was important to

assess how its functional capacity was distributed across these joints. In other words, it was important to determine whether there was architectural specialization within latissimus dorsi. To accomplish this, each muscle was divided regionally (Fig. 1) and the architecture of each region was quantified (Table 1, Fig. 2). This analysis showed that the LPC region constitutes approximately 64% of the total physiological cross-sectional area of the entire muscle ($PCSA = 3.6 \pm 0.3 \text{ cm}^2$), whereas the thoracic region constitutes approximately 36% ($PCSA = 2.0 \pm 0.2 \text{ cm}^2$). This indicates that nearly two-thirds of the force-generating capability of the latissimus dorsi muscle resides within the LPC region. From a functional point of view, the greater stabilizing potential of the muscle within the lumbar region can be considered a positive design feature, with a potentially negative trade-off of imposing greater loads to this region of the spine.

Measured sarcomere length, in the neutral spine post-mortem state, was essentially optimal at $2.69 \mu\text{m}$ ($2.75 \mu\text{m}$ for the thoracic region; $2.63 \mu\text{m}$ for the LPC region), indicating that this muscle is at optimal force-generating length in the neutral position. Modelled length changes across the spine ROM predict that both thoracic and LPC fibres of latissimus dorsi deviate only modestly from optimal force-generating length through the range of flexion to extension, as well as ipsilateral to contralateral twist, and therefore would maintain their ability to generate nearly maximal isometric force over the full ROM about each of these anatomic spine axes. Conversely, modelled length changes predict that fibres undergo much larger deviations from optimal length in lateral bend of the spine, particularly those in the LPC region. As the spine bends laterally to the ipsilateral side, fibres in this region become progressively shorter, with sarcomeres decreasing to lengths as short as $1.64 \mu\text{m}$ (at which point the muscle fibres would only be capable of generating approximately 60% of their maximum force); as the spine bends laterally to the contralateral side, fibres become progressively longer, with sarcomeres increasing to lengths up to $3.30 \mu\text{m}$ (at which point the muscle fibres would only be capable of generating approximately 70% of their maximum force). Fibres in the thoracic region were predicted to behave in a similar manner, although sarcomere length changes, and thus impairment of force production, are less substantial (Fig. 3A). Nonetheless, these data indicate that the force-generating capacity of latissimus dorsi decreases progressively as the spine is bent laterally to both the ipsilateral and contralateral sides, such that it is weakest at the end lateral bend ROM. From a functional point of view, this is less than ideal, as it creates a situation in which the restoring force of latissimus dorsi muscle becomes weaker (particularly in the lumbar region) with increasing deflection from neutral. That being said, the data presented here do not account for passive tension, which can play a role in providing resistive force during muscle lengthening (Lieber & Bodine-Fowler,

1993). Therefore, although the lengthened latissimus dorsi muscle will have a weakened ability to generate active force due to decreased myofilament overlap, the presence of passive forces may help to compensate for some of the restoring force that is lost during contralateral bend. Modelled length changes of latissimus dorsi over full range of motion about two of the anatomic shoulder axes demonstrate that fibres from both the thoracic and LPC regions operate on or near the plateau region of the force-length curve during shoulder extension and adduction. During flexion and abduction, fibres within both regions of the muscle progressively lengthen; sarcomeres in the thoracic region increase to lengths up to approximately $3.33 \mu\text{m}$ (at which point the muscle fibres would only be capable of generating approximately 70% of their maximum force), whereas sarcomeres within the LPC region extend to lengths up to $3.12 \mu\text{m}$ (at which point fibres would be capable of generating approximately 85% of their maximum force) (Fig. 3B). These data indicate that, as in lateral bend of the spine, the force-generating capacity of latissimus dorsi becomes progressively weaker in flexion and abduction as the arm deviates further from anatomical position. By corollary, this will also lead to a progressive weakening of its force-generating and stabilizing capacity at the spine. Interestingly, predicted sarcomere length operating ranges across shoulder ROM suggest that the decrease in force-generating capability during flexion and abduction of the shoulder will affect the thoracic spine to a greater extent than the lumbar spine. Modelled operating ranges indicate that sarcomeres within the thoracic region of latissimus dorsi reach lengths that are approximately $0.21 \mu\text{m}$ longer during full flexion and abduction than sarcomeres within the LPC region, which equates to an approximately 15% greater reduction in force-generating capacity for the thoracic fibres compared with LPC fibres. From a functional spine viewpoint this design feature may be considered favourable, as it suggests that during movement of the arm at the shoulder joint, the force-generating capacity of latissimus dorsi is conserved to a greater extent in the region of the muscle that attaches to the lumbar spine.

Biomechanical models rely heavily on muscle architectural data and mechanical properties to predict muscle forces and joint forces of simulated body movements (Hansen et al. 2006). Prior to the current study, detailed information regarding the architecture and mechanical function of the latissimus dorsi muscle was limited, yet many biomechanical models, specifically those designed to predict muscle forces, and assess loading and stability of the lumbar spine, have incorporated latissimus dorsi in their analyses (McGill & Norman, 1986; McGill, 1987; Potvin et al. 1991; Goel et al. 1993; Cholewicki et al. 1995; Granata & Marras, 1995; Cholewicki & McGill, 1996; Guzik et al. 1996; Marras & Granata, 1997). Of particular importance for the effective use of these models are accurate estimates of individual muscle PCSA, which are used to predict forces applied to

the lumbar spine (Brown & Gerling, 2012). Bogduk et al. (1998) previously reported a PCSA of 6.2 cm² of the latissimus dorsi muscle, based on estimates from five elderly cadavers. This is comparable to the PCSA value of 5.6 cm² reported here, most likely due to the lengths of sarcomeres within the latissimus dorsi being near optimal in the cadaveric neutral spine position (2.69 µm measured here). When quantifying muscle architecture, it is important to compensate for potential lengthening or shortening of muscles that may occur during fixation (Lieber & Friden, 2000); not doing so could result in PCSA estimations that are based on measurements of muscles in either thinned or thickened states, subsequently leading to under- and over-estimations of these values, respectively (Brown & Gerling, 2012). Thus, this study has demonstrated that because sarcomere lengths measured within the latissimus dorsi are near optimal in a cadaveric neutral position, the previously reported PCSA values of Bogduk et al. (1998) most likely accurately represent the force-generating potential of the latissimus dorsi.

An unexpected finding in the present study was that the latissimus dorsi muscles fixed in a lengthened state had a mean sarcomere length (2.64 ± 0.04 µm) that was virtually the same as that of 'non-stretched' muscles (2.69 ± 0.06 µm), despite their substantially longer fascicles (it should be noted that these lengths are representative of sarcomeres located more centrally within the latissimus dorsi muscle). Based on this finding, we hypothesized that, due to the high number of sarcomeres arranged in series within the latissimus dorsi muscle, not all sarcomeres were stretched to the same degree during whole muscle lengthening; therefore, as it appeared that sarcomeres located more centrally within the muscle were unaffected by whole muscle lengthening, sarcomeres closer to the ends of the muscle would be found to be stretched.

To test this hypothesis, samples were taken from near the humeral insertion tendon of the stretched latissimus dorsi muscles, and sarcomeres were measured as described earlier. Surprisingly, these sarcomeres were found to be even shorter, having an average length of 2.38 ± 0.03 µm ($n = 3$ donors). We present two potential reasons for this surprising finding. First, previous research has shown that in many long feline muscles, fibres do not run the entire length of the muscle or even the entire length of the fascicle; rather, these muscles are composed of relatively short fibres arranged in an overlapping longitudinal series within the muscle (Loeb et al. 1987; Ounjian et al. 1991; Trotter & Purslow, 1992). This fibre arrangement has also been suggested in human skeletal muscle (Woodley et al. 2007) including the latissimus dorsi (Snobl et al. 1998). In this case, one might hypothesize that, rather than leading to sarcomere stretching, lengthening of the muscle prior to fixation caused the short overlapping muscle fibres within latissimus dorsi to slide with respect to one another, leaving the sarcomeres relatively unaffected. However, further analysis of the fibre arrangement and mechanics of latissimus dorsi is

necessary to verify this hypothesis. Alternatively, it is possible that muscle fibres were simply damaged and torn when abducting the arms prior to the embalming process, thus causing the muscle fibres to shorten towards their slack length. This would account for the relatively unexpected short sarcomere lengths measured in these 'stretched' muscles.

There are several considerations pertaining to the data reported here that must be addressed. First, by force of circumstance, most of the cadaveric specimens used in the present study were elderly, which is unfortunately a common limitation of cadaveric studies of muscle architecture. It is well known that skeletal muscle atrophies with increasing age (Faulkner et al. 2007), and thus it is possible that the PCSA values reported here may underestimate those found in younger adults. However, it should be noted that the latissimus dorsi muscles from which PCSA was quantified came from cadavers ranging from 48 to 83 years of age (Table 1); therefore, it could be argued that the PCSA values reported here are, to a certain extent, representative of the adult population as a whole. Additionally, the average age of the cadaveric specimens was 68.3 ± 11.0 years (Table 1), which is considerably younger than the average age of donors reported in other cadaveric studies of trunk muscle architecture (77.7 ± 16.3 years; Brown et al. 2010, and 84.0 ± 3.0 years; Ward et al. (2009).

Second, calculation of sarcomere operating ranges did not take into account potential tendon compliance. The magnitude of muscle fibre length change during stretching or shortening is in part dependent upon the compliance of its in-series tendon. With regard to the latissimus dorsi muscle, although its tendon of insertion onto the humerus is relatively short, the thoracolumbar fascia that attaches this muscle to the spine and ilium consists of a considerable amount of tendinous tissue, particularly in the lumbar and sacral regions. Future work is therefore needed to assess the impact of this tendon length-muscle fibre length ratio on the functional capacity of this muscle.

Third, due to the complexity of the shoulder joint and the unique corkscrew design of the humeral insertion of latissimus dorsi, sarcomere length operating range was not modelled for internal/external rotation of the shoulder.

Finally, sarcomere length operating ranges of latissimus dorsi were modelled across spine and shoulder ROM independently. However, due to the complex inter-relationship of the various segments of the body during movement, it is unrealistic to think that the spine and shoulder function independently of one another. Therefore, further work is necessary to determine the force-length characteristics of the latissimus dorsi muscle during simultaneous movement of the spine and shoulder.

The architectural data reported here provide an improved understanding of the functional capacity of the latissimus dorsi muscle. Of equal importance, measurement of sarcomere length allowed for the estimation of sarcomere

length operating ranges across the spine and shoulder ROM, providing for the first time these detailed insights into the mechanical function of the latissimus dorsi muscle. Future work is needed to elucidate specifics regarding the role of latissimus dorsi on the interplay between spine and shoulder function.

Acknowledgements

We thank Dr Lorraine Jadeski and Premila Sathasivam for their cooperation in obtaining study specimens. We also thank Alyssa Runyon, Navneet Shergill, Olesya Oligradska, and Elizabeth Byrne for their help in preparing muscles for analysis, as well as with their assistance in data collection.

Authors' contributions

M.E.G. prepared study specimens, collected the architectural data, and wrote the manuscript. S.H.M.B. designed the study, prepared modelling data, and contributed to the revision of the manuscript. Both authors contributed to data analysis and interpretation.

References

- Adams M, Bogduk N, Burton K, et al. (2002) *The Biomechanics of Back Pain*. Amsterdam: Elsevier Science Limited.
- Bodine SC, Roy RR, Meadows DA, et al. (1982) Architectural, histochemical, and contractile characteristics of a unique biarticular muscle: the cat semitendinosus. *J Neurophysiol* **48**, 192–201.
- Bogduk N, Johnson G, Spalding D (1998) The morphology and biomechanics of latissimus dorsi. *Clin Biomech* **13**, 377–385.
- Brown SHM, Gerling ME (2012) Importance of sarcomere length when determining muscle physiological cross-sectional area: a spine example. *Proc Inst Mech Eng H* **226**, 384–388.
- Brown SHM, Potvin JR (2007) Exploring the geometric and mechanical characteristics of the spine musculature to provide rotational stiffness to two spine joints in the neutral posture. *Hum Mov Sci* **26**, 113–123.
- Brown SHM, Ward SR, Cook MS, et al. (2010) Architectural analysis of human abdominal wall muscles – implications for mechanical function. *Spine* **36**, 355–362.
- Cholewicki J, McGill SM (1996) Mechanical stability of the in vivo lumbar spine: implications for injury and chronic low back pain. *Clin Biomech* **11**, 1–15.
- Cholewicki J, McGill SM, Norman RW (1995) Comparison of muscle forces and joint load from an optimization and EMG assisted lumbar spine model: towards development of a hybrid approach. *J Biomech* **28**, 321–331.
- Delp SL, Loan JP (1995) A graphics-based software system to develop and analyze models of musculoskeletal structures. *Comput Biol Med* **25**, 21–34.
- Delp SL, Suryanarayanan S, Murray WM, et al. (2001) Architecture of the rectus abdominis, quadratus lumborum, and erector spinae. *J Biomech* **34**, 371–375.
- Faulkner JA, Larkin LM, Claflin DR, et al. (2007) Age-related changes in the structure and function of skeletal muscles. *Clin Exp Pharmacol Physiol* **34**, 1091–1096.
- Goel VK, Kong W, Han JS, et al. (1993) A combined finite element and optimization investigation of lumbar spine mechanics with and without muscles. *Spine* **11**, 1531–1541.
- Gordon AM, Huxley AF, Julian FJ (1966) The variation in isometric tension with sarcomere length in vertebrate muscle fibres. *J Physiol* **184**, 170–192.
- Granata KP, Marras WS (1995) An EMG-assisted model of trunk loading during free dynamic lifting. *J Biomech* **28**, 1309–1317.
- Guzik DC, Keller TS, Szpalski M, et al. (1996) A biomechanical model of the lumbar spine during upright isometric flexion, extension, and lateral bending. *Spine* **21**, 427–433.
- Hansen S, de Zee M, Rasmussen J, et al. (2006) Anatomy and biomechanics of the back muscles in the lumbar spine with reference to biomechanical modelling. *Spine* **31**, 1888–1899.
- Lieber RL, Bodine-Fowler SC (1993) Skeletal muscle mechanics: implications for rehabilitation. *Phys Ther* **73**, 844–856.
- Lieber RL, Friden J (2000) Functional and clinical significance of skeletal muscle architecture. *Muscle Nerve* **23**, 1647–1666.
- Lieber RL, Friden J (2001) Clinical significance of skeletal muscle architecture. *Clin Orthop Relat Res* **383**, 140–151.
- Lieber RL, Fazeli BM, Botte MJ (1990) Architecture of selected wrist flexor and extensor muscles. *J Hand Surg Am* **15**, 244–250.
- Loeb GE, Pratt CA, Chanaud CM, et al. (1987) Distribution and innervation of short, interdigitated muscle fibers in parallel-fibered muscles of the cat hindlimb. *J Morphol* **191**, 1–15.
- Marras WS, Granata KP (1997) Spine loading during trunk lateral bending motions. *J Biomech* **30**, 697–703.
- McGill SM (1987) A biomechanical perspective of sacro-iliac pain. *Clin Biomech* **2**, 345–351.
- McGill SM (2002) *Low Back Disorders: Evidence-Based Prevention and Rehabilitation*. Champaign: Human Kinetics Publishers.
- McGill S, Norman RW (1986) Partitioning of the L4-L5 dynamic moment into disc, ligamentous, and muscular components during lifting. *Spine* **11**, 666–678.
- Namdari S, Yagnik G, Edbaugh DD, et al. (2012) Defining functional shoulder range of motion for activities of daily living. *J Shoulder Elbow Surg* **21**, 1177–1183.
- Ounjian M, Roy RR, Eldred E, et al. (1991) Physiological and developmental implications of motor unit anatomy. *J Neurobiol* **22**, 547–559.
- Potvin JR, McGill SM, Norman RW (1991) Trunk muscle and lumbar ligament contributions to dynamic lifts with varying degrees of flexion. *Spine* **16**, 1090–1107.
- Powell PL, Roy RR, Kanim P, et al. (1984) Predictability of skeletal muscle tension from architectural determinations in guinea pig hindlimbs. *J Appl Physiol* **57**, 1715–1721.
- Rassier DE, MacIntosh BR, Herzog W (1999) Length dependence of active force production in skeletal muscle. *J Appl Physiol* **86**, 1445–1457.
- Schultz AB, Andersson GB (1981) Analysis of loads on the lumbar spine. *Spine* **6**, 76–82.
- Snobli D, Binaghi LD, Zenker W (1998) Microarchitecture and innervations of the human latissimus dorsi muscle. *J Reconstr Microsurg* **14**, 171–173.
- Trotter JA, Purslow PP (1992) Functional morphology of the endomysium in series fibered muscles. *J Morphol* **212**, 109–122.
- Walker SM, Schrodt GR (1974) I segment lengths and thin filament periods of skeletal muscle fibers of the rhesus monkey and the human. *Anat Rec* **178**, 63–82.

Ward SR, Lieber RL (2005) Density and hydration of fresh and fixed human skeletal muscle. *J Biomech* **38**, 2317–2320.

Ward SR, Kim CW, Eng CM, et al. (2009) Architectural analysis and intraoperative measurements demonstrate the unique design of the multifidus muscle for lumbar spine stability. *J Bone Joint Surg Am* **91**, 176–185.

White AA, Panjabi MM (1990) *Clinical Biomechanics of the Spine*, 2nd edn. Philadelphia: J.B. Lippincott Company.

Woodley SJ, Duxson MJ, Mercer SR (2007) Preliminary observations on the microarchitecture of the human abdominal wall muscles. *Clin Anat* **20**, 808–813.